nature genetics

Loss-of-function mutations of an inhibitory upstream ORF in the human hairless transcript cause Marie Unna hereditary hypotrichosis

Yaran Wen[1,21], Yang Liu[2,21], Yiming Xu[1,21], Yiwei Zhao[3,21], Rui Hua[1], Kaibo Wang[4], Miao Sun[1], Yuanhong Li[4], Sen Yang[5], Xue-Jun Zhang[5], Roland Kruse[6], Sven Cichon[7,8], Regina C Betz[7], Markus M Nöthen[7,8], Maurice A M van Steensel[9], Michel van Geel[9], Peter M Steijlen[9], Daniel Hohl[10], Marcel Huber[10], Giles S Dunnill[11], Cameron Kennedy[11], Andrew Messenger[12], Colin S Munro[13], Alessandro Terrinoni[14], Alain Hovnanian[15], Christine Bodemer[16], Yves de Prost[16], Amy S Paller[17], Alan D Irvine[18,19], Rod Sinclair[20], Jack Green[20], Dandan Shang[1], Qing Liu[1], Yang Luo[2], Li Jiang[2], Hong-Duo Chen[4], Wilson H-Y Lo[1], W H Irwin McLean[3], Chun-Di He[4] & Xue Zhang[1,2]

Marie Unna hereditary hypotrichosis (MUHH) is an autosomal dominant form of genetic hair loss. In a large Chinese family carrying MUHH, we identified a pathogenic initiation codon mutation in *U2HR*, an inhibitory upstream ORF in the 5′ UTR of the gene encoding the human hairless homolog (*HR*). *U2HR* is predicted to encode a 34–amino acid peptide that is highly conserved among mammals. In 18 more families from different ancestral groups, we identified a range of defects in *U2HR*, including loss of initiation, delayed termination codon and nonsense and missense mutations. Functional analysis showed that these classes of mutations all resulted in increased translation of the main *HR* physiological ORF. Our results establish the link between MUHH and *U2HR*, show that fine-tuning of HR protein levels is important in control of hair growth, and identify a potential mechanism for preventing hair loss or promoting hair removal.

Hair follicles, the mini-organs where periodic hair growth and shedding occur, show a remarkable capacity for cyclic regeneration. The dynamic hair cycle, consisting of the sequential anagen (the normal rapid-growth phase with active cell proliferation, migration and differentiation), catagen (a regressive phase with prominent apoptosis) and telogen (a quiescent phase)[1,2], is thought to be mediated by epithelial stem cells located in the hair follicle bulge region[3]. Most hair loss (alopecia, atrichia and hypotrichosis) and excessive hair growth (hypertrichosis and hirsutism) seen in clinical practice are the results of changes in hair follicle cycling[1].

The Wnt signaling pathway coordinates with many factors in initiating the neogenesis and regeneration of hair follicles[4–8]. *HR* encodes a nuclear receptor corepressor that can directly repress expression of the Wnt inhibitors Wise and Soggy, thereby regulating the timing of Wnt signaling required for hair follicle cycling and activating the regeneration of hair follicles[9–11]. Loss-of-function mutations in *HR* can lead to autosomal recessive congenital atrichia (OMIM 203655, 209500)[12–14]. MUHH (OMIM 146550), an autosomal dominant form of genetic hair loss, was first described by the German dermatologist Marie Unna[15] and is characterized by sparse or absent hair at birth, growth of coarse and wiry hair during childhood and progressive hair loss at puberty. The MUHH locus has been mapped to 8p21, the chromosomal region harboring *HR*, by several research

[1]McKusick-Zhang Center for Genetic Medicine and National Laboratory of Medical Molecular Biology, Institute of Basic Medical Sciences, Chinese Academy of Medical Sciences & Peking Union Medical College, Beijing 100005, China. [2]The Research Center for Medical Genomics, China Medical University, Shenyang 110001, China. [3]Epithelial Genetics Group, Division of Molecular Medicine, Colleges of Life Sciences and Medicine, Dentistry & Nursing, University of Dundee, Dundee DD1 5EH, Scotland, UK. [4]Department of Dermatology, No. 1 Hospital of China Medical University, Shenyang 110001, China. [5]Institute of Dermatology, Anhui Medical University, Hefei 230032, China. [6]Department of Dermatology, University of Düsseldorf, D-40225 Düsseldorf, Germany. [7]Institute of Human Genetics, University of Bonn, D-53111 Bonn, Germany. [8]Department of Genomics, Life & Brain Center, University of Bonn, D-53127 Bonn, Germany. [9]Maastricht University Center for Molecular Dermatology, University Hospital Maastricht, 6202AZ Maastricht, The Netherlands. [10]CHUV, Hôpital de Beaumont, CH-1011 Lausanne, Switzerland. [11]Department of Dermatology, Bristol Royal Infirmary, Bristol BS2 8HW, UK. [12]Department of Dermatology, Royal Hallamshire Hospital, Sheffield S10 2JF, UK. [13]Department of Dermatology, Southern General Hospital, Glasgow G51 4TF, UK. [14]IDI-IRCCS Biochemistry Laboratory, University of Tor Vergata, 00133 Rome, Italy. [15]INSERM U563, Centre de Physiopathologie de Toulouse Purpan, Toulouse F-313000, France. [16]Department of Dermatology, Necker Hospital, 75105 Paris, France. [17]Departments of Dermatology and Pediatrics, Northwestern University, Chicago, Illinois 60611, USA. [18]Department of Paediatric Dermatology, Our Lady's Children's Hospital, Dublin 12, Ireland. [19]Department of Clinical Medicine, Trinity College Dublin, Dublin 2, Ireland. [20]Department of Dermatology, St. Vincent's Hospital, Melbourne, Victoria 3065, Australia. [21]These authors contributed equally to this work. Correspondence should be addressed to X.Z. (xuezhang@pumc.edu.cn), W.H.I.M. (w.h.i.mclean@dundee.ac.uk) or C.-D.H. (chundihe@hotmail.com).

Received 8 August 2008; accepted 14 October 2008; published online 4 January 2009; doi:10.1038/ng.276

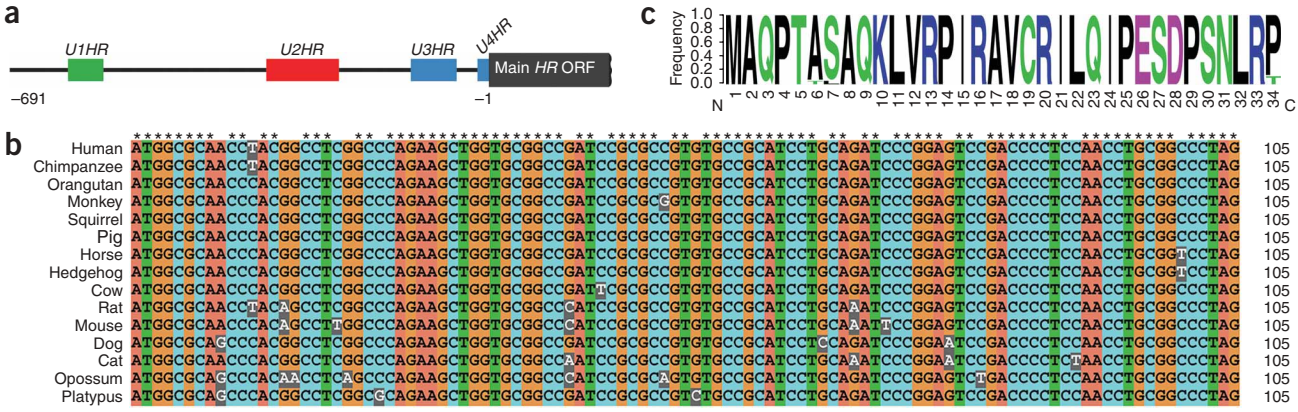

Figure 1 The 5′ UTR of *HR* contains a highly conserved upstream ORF. (**a**) *HR* 5′ UTR (–691 to –1), showing position and size of the four upstream ORFs. (**b**) Alignment of 15 mammalian *U2HR* nucleic acid sequences. Identical nucleotides are indicated by asterisks. Numbers on right indicate sizes. (**c**) Amino acid sequence logo of 15 aligned *U2HR*-encoded polypeptides predicted from the 15 mammalian *U2HR* nucleic acid sequences. Amino acids are indicated as single letters and numbered. N, N terminus; C, C terminus. Acidic, basic, hydrophobic and polar amino acids are colored purple, blue, black and green, respectively. Vertical axis shows residue frequencies, represented by the height of the individual letters. Invariant residues have a frequency of 1.

groups using families from various ancestral groups[16–20]. However, the gene responsible for MUHH has not yet been discovered.

Mutations affecting mRNA translation have been documented in many genetic diseases[21]. Upstream ORFs in the 5′ UTR of an mRNA transcript can modulate the translational efficiency of the main ORF, and disruptions of a functional upstream ORF have been associated with human genetic diseases[22–24]. Mouse hair follicles in anagen have *Hr* mRNA but not protein expression[10,25], suggesting the presence of expression regulation at the translational level. Previous sequence analyses in families with MUHH were unable to identify any pathogenic mutations in the coding region of *HR*[16–20]. We therefore postulated that mutations in a *cis*-acting translational regulator outside the *HR* coding region, such as an upstream ORF, are the cause of MUHH.

We carried out bioinformatics analysis using the UCSC Genome Browser and found that the reference sequence of human *HR* deposited in the NCBI RefSeq database is incomplete. The RefSeq *HR* cDNA has a 5′ UTR of 130 nt. On the basis of the existence of many ESTs aligned to the genomic region of *HR* exon 1 (**Supplementary Fig. 1** online) and our sequence analysis of the RT-PCR fragments produced in the A375 and HeLa cell lines (**Supplementary Fig. 2** online), we were able to extend the 5′ UTR to 691 nt (**Fig. 1a**

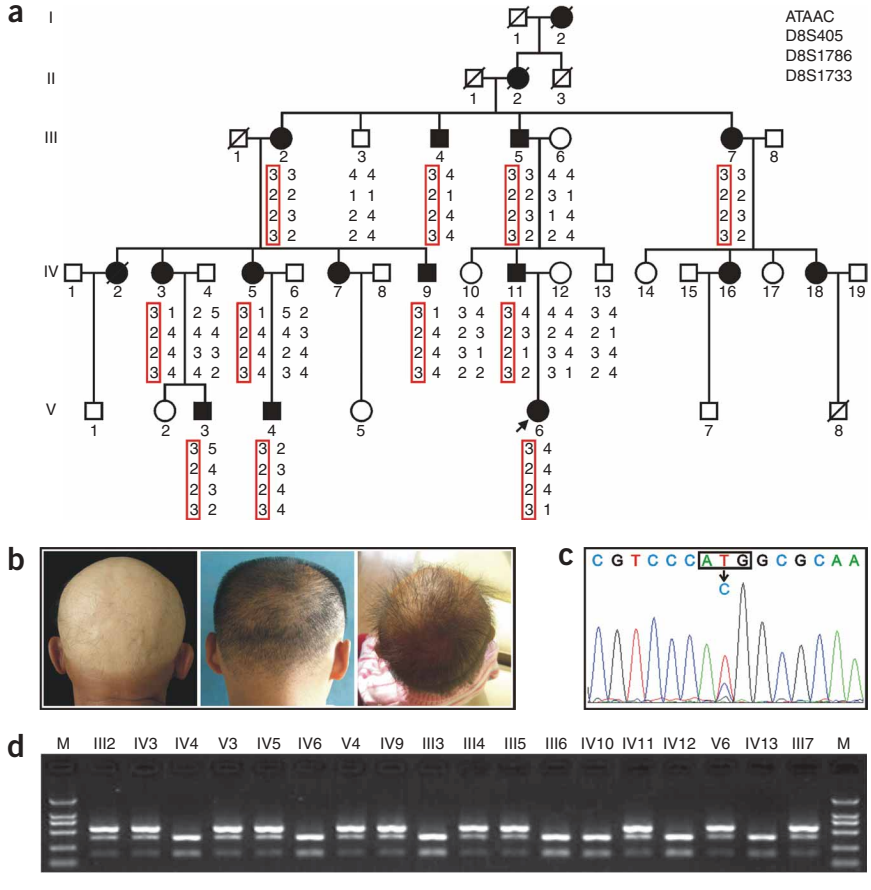

Figure 2 Initial identification of the 2T>C (no protein produced) *U2HR* mutation in a large Chinese family with MUHH. (**a**) Pedigree and disease haplotype segregation. Filled symbols represent affected individuals with MUHH; open symbols represent individuals with a normal hair phenotype. Circles and squares indicate females and males, respectively. The disease haplotype is boxed. (**b**) Hair growth defect in affected individuals of the Chinese family. Examples show almost-complete alopecia in a 56-year-old male (III5; left), coarse and wiry hair in a 17-year-old boy (V4; middle) and sparse hair in a 6-year-old girl (V6; right). (**c**) Sequencing chromatogram showing heterozygous 2T>C initiation codon mutation in *U2HR*. (**d**) *Nco*I restriction analysis indicates segregation of the 2T>C mutation, shown as a 538-bp fragment, with the disease phenotype in the family. A PCR fragment of 538 bp was first produced by the PCR using the HRUP3F1 and HRUP3R1 primers and then digested with the *Nco*I enzyme. The fragment can be cut into two fragments (368 bp and 170 bp) in the wild type but not in the mutant. M, DNA marker.

Table 1 U2HR mutations identified in 19 families with MUHH

Mutation	Protein alteration	Number of unrelated families	Ancestral groups	Reference
1A>G	0	2	Australian	This study
			British	This study
1A>T	0	1	Swiss	This study
2T>A	0	1	Swiss	This study
2T>C	0	3	American	18
			Belgian	19
			Chinese	This study
3G>A	0	1	American	This study
7C>T	Q3X	1	English	17
20C>A	S7X	1	German	This study
71T>A	I24N	1	Dutch	17
73C>G	P25A	3	Dutch	17
			English	19
			Italian	This study
76G>A	E26K	1	French	19
82G>C	D28K	1	Scottish	This study
103T>C	X35Qext1263X	1	German	20
104A>G	X35Wext1263X	2	Chinese	21
			Chinese	This study

and **Supplementary Fig. 3** online). We found four upstream ORFs in the *HR* 5′ UTR, designated *U1HR*, *U2HR*, *U3HR* and *U4HR*, from 5′ to 3′ (**Fig. 1a** and **Supplementary Fig. 3**). Multiple alignment analysis of all available mammalian sequences showed that the proximal (*U1HR*), the longest (*U2HR*) and the shortest (*U4HR*) are conserved both in sequence and size (**Fig. 1b** and **Supplementary Fig. 4** online). *U2HR* specifies a highly conserved peptide of 34 amino acids, of which 31 are invariant in all 15 known mammalian sequences (**Fig. 1c**).

The presence of upstream ORFs in the *HR* 5′ UTR raised the possibility that MUHH is caused by mutations in one of these. To address this question, we carried out two-point linkage analysis using four microsatellite markers flanking the *HR* locus in a large Han Chinese family with MUHH and confirmed the genetic mapping to chromosome 8p21 (**Fig. 2a**,**b**). We sequenced genomic DNA from an affected individual for three candidate genes, *FGF17*, *HR* and *FAM160B2*, and identified an initiation codon mutation (2T>C) in the *U2HR* cDNA (**Fig. 2c**). The mutation eliminates the only ATG codon of *U2HR*, which is most likely to lead to complete loss of protein translation. By restriction analysis using *Nco*I, this mutation was confirmed in all affected individuals but was not detected in unaffected family members or in 617 unrelated Han Chinese control subjects (**Fig. 2d**). In 18 more families with a confirmed clinical diagnosis of MUHH, including 8 in which genetic linkage to 8p21 had been described previously[16–20], we identified further mutations in *U2HR*. In all, we detected 13 distinct *U2HR* mutations in 19 families from different ancestral groups (**Table 1**). All pathogenic mutations were single-base substitutions, and seven of them were at the initiation or termination codons of *U2HR*, leading to loss-of-initiation or delayed termination codon mutations, respectively. With the exception of two nonsense mutations, all of the other mutations were missense. This mutation spectrum, particularly the presence of missense and delayed termination codon mutations, strongly suggests that *U2HR* encodes a functional peptide and that the MUHH-causing mutations are essentially loss-of-function mutations. Notably, all missense mutations were found in codons 24–28 of *U2HR*, suggesting the functional importance of the corresponding amino acid residues. We did not observe obvious genotype-phenotype correlation in these 19 families with MUHH. We analyzed the entire 5′ UTR and identified no mutations in a further six families with MUHH. In these cases, the referring clinicians had also seen families with MUHH with *U2HR* mutations reported here, and the phenotype was virtually indistinguishable from *U2HR*-related MUHH. In one larger kindred, the *HR* locus was fully excluded by linkage analysis (data not shown), as was the recently reported 1q locus for a MUHH-like disorder[26]. Thus, there seems to be at least one other gene in which mutations closely phenocopy MUHH.

To determine whether *U2HR* can modulate translation of the downstream main *HR* ORF, we inserted the 5′ UTR (–642 to –1) and the first 27 codons into a pGL3 reporter vector to drive translation of a fused HR–firefly luciferase protein (**Fig. 3a**). We individually changed the initiation codon of each upstream ORF to

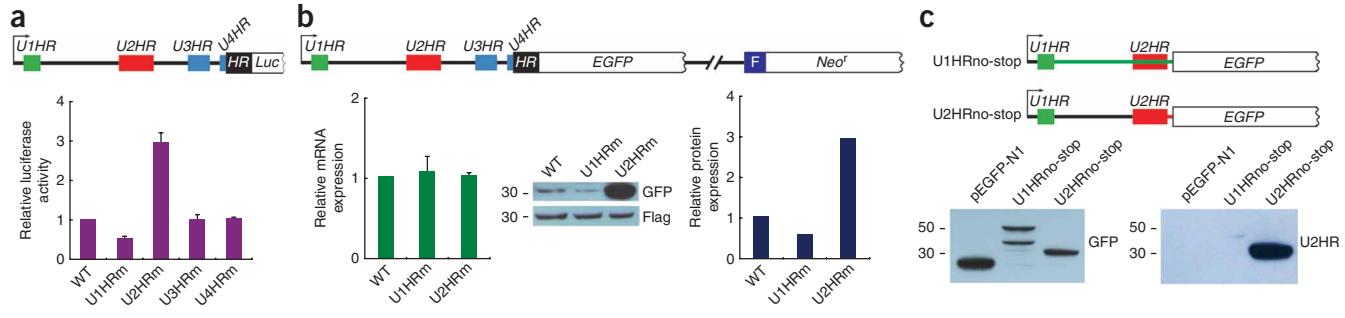

Figure 3 *U2HR* has an inhibitory effect on translation of the downstream main *HR* ORF. (**a**) HR-luciferase reporter construct, with *HR* 5′ UTR. Graph shows relative reporter activity of wild type (WT) and mutants with T>C mutation in ATG codon. Compared to WT, U1HRm, U2HRm, U3HRm and U4HRm showed relative luciferase activity of 0.49 ± 0.09, 2.95 ± 0.26, 0.99 ± 0.15 and 1.01 ± 0.06, respectively. (**b**) HR-EGFP expression construct, with *HR* 5′ UTR. Shown below are expression analyses of the U1HRm and U2HRm mutants. F represents triple Flag tag; Neo^r represents neomycin phosphotransferase selection marker. Lower left, quantitative real-time RT-PCR shows similar relative HR-EGFP mRNA expression level in cells transfected with WT, U1HRm or U2HRm construct. Lower middle, immunoblots with antibody to Flag or GFP show altered HR-EGFP protein level in cells transfected with the U1HRm and U2HRm mutants. Lower right, cells transfected with the U1HRm and U2HRm mutants have relative HR-EGFP protein expression levels of 0.56 and 2.91, respectively, compared to WT. These alterations are consistent with changes in HR-luciferase reporter activity. (**c**) Translation initiation at *U1HR* and *U2HR*. Top, U1HRno-stop and U2HRno-stop expression constructs, showing in-frame fusions of *U1HR* or *U2HR* with ORF encoding EGFP. Left, immunoblot with antibody to GFP shows expression of the fused proteins with a molecular weight higher than that of EGFP of the parental pEGFP-N1 control. Right, immunoblot with antibody to U2HR validates translation of the U2HR-EGFP protein. Error bars, s.d.

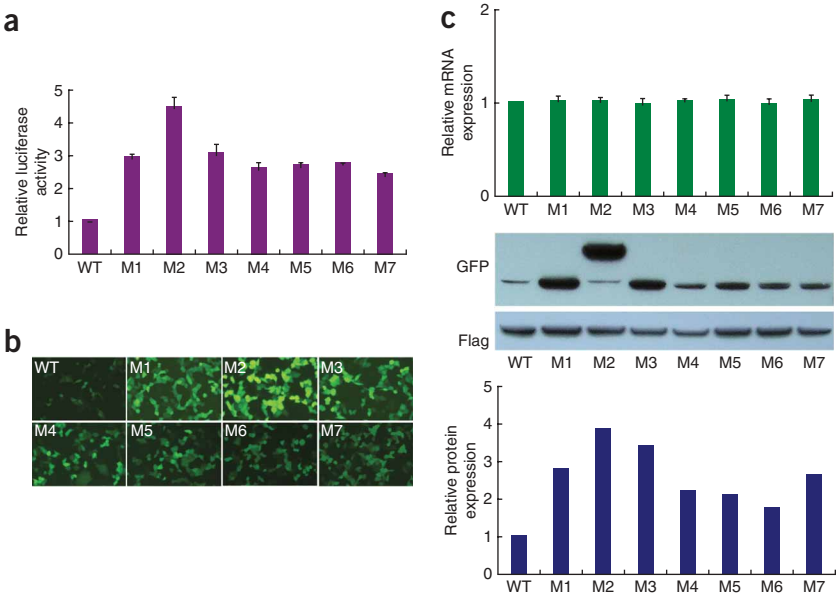

Figure 4 Mutations in *U2HR* abolish its inhibitory effect on *HR* translation. (**a**) Cells transfected with HR-luciferase reporter constructs containing *U2HR* mutations all have increased luciferase activity. (**b**) Cells transfected with HR-EGFP expression constructs containing *U2HR* mutations all show enhanced fluorescent signal. (**c**) Cells transfected with HR-EGFP expression constructs all show a similar relative HR-EGFP mRNA expression level (top), but those with MUHH-causing *U2HR* mutations show increased relative HR-EGFP protein expression (middle and bottom). WT, wild-type; M1, 2T>C (no protein produced); M2, 104A>G (X35Wext1163X); M3, 7C>T (Q3X); M4, 71T>A (I24N); M5, 73C>G (P25A); M6, 82G>C (D28H); M7, 76G>A (E26K). Error bars, s.d.

ACG by PCR-mediated mutagenesis. Our reporter assays in HeLa cells using these plasmids showed that only two mutations resulted in significant changes in relative luciferase activity ($P < 0.001$). The *U1HR* mutant retained about half of the luciferase activity, and the mutation in *U2HR* caused a threefold increase in luciferase activity compared to wild type (**Fig. 3a**), suggesting that *U1HR* and *U2HR* function as stimulatory and inhibitory translational control elements, respectively.

We then transferred these reporter constructs into a green fluorescent protein (GFP) vector expressing Flag-tagged neomycin phosphotransferase (Neo^r) to place the *HR* coding region in frame with the downstream ORF encoding enhanced GFP (EGFP; **Fig. 3b**). We transfected these constructs individually into HeLa cells and conducted quantitative real-time RT-PCR and immunoblot analyses. The two mutations clearly affected protein translation, but not mRNA expression (**Fig. 3b**). We also generated mutant constructs with *U1HR* or *U2HR* fused in frame to the EGFP-encoding ORF and observed efficient translation of the two upstream ORFs in transfected cells (**Fig. 3c**). We verified the translation of *U2HR* using a polyclonal antibody to U2HR (**Fig. 3c**). Taken together, the functional *U1HR* and *U2HR* seem to encode active peptides and can positively and negatively regulate protein translation of the main *HR* physiological ORF, respectively.

To further investigate the functional effects of the pathogenic mutations identified in *U2HR*, we used the fused HR–firefly luciferase reporter and HR-EGFP expression constructs (**Fig. 3a**,**b**) containing the *HR* 5′ UTR with wild-type or mutant *U2HR*. We selected seven representative *U2HR* mutations: one at the initiation codon, one at the termination codon, one nonsense and four missense. Cells transfected with the mutant constructs showed greater luciferase activity than did cells transfected with the wild-type construct (**Fig. 4a**). Consistent with this observation, all of the cells transfected with the HR-EGFP expression plasmids containing mutated *U2HR* showed an enhanced fluorescent signal (**Fig. 4b**). Using quantitative real-time RT-PCR and immunoblotting, we confirmed that all mutations resulted in augmented expression of the HR-EGFP protein, whereas mRNA expression showed no significant difference between the wild-type and the mutants (**Fig. 4c**). These results suggested that the MUHH-causing mutations lead to increased translation of the main *HR* ORF. Notably, the X35Wext1163X delayed termination codon mutation, which is predicted to result in an in-frame *U2HR-HR* fused ORF, caused increased translation of HR-EGFP with higher molecular weight, further confirming the translational competence of *U2HR*.

Disruption of an upstream ORF represents a mutational mechanism recently identified in human genetic disease[21,22]. Upstream ORFs are common in the 5′ UTRs of human mRNA transcripts[27,28]; a human 5′ UTR longer than 400 nt contains on average four upstream ORFs[27]. The importance of these translational regulators in molecular pathogenesis may have been overlooked while screening for pathogenic mutations underlying human genetic diseases; previous genetic mapping and mutation screening in MUHH, for example, was focused on the coding exons of *HR*[16–20]. We found four upstream ORFs in the *HR* 5′ UTR and showed that two of them, *U1HR* and *U2HR*, exert regulatory effects on translation of the downstream main ORF. Of note, we identified MUHH-causing mutations only in the inhibitory *U2HR*, but our results do not exclude involvement of the positive-acting *U1HR* in other hair phenotypes.

Many inhibitory upstream ORFs may simply function as a translational barrier by blocking the scanning ribosomes from reaching the initiation codon of the downstream ORF[29]. As shown in hereditary thrombocythemia and familial cutaneous melanoma[23,24], removal and creation of a barrier upstream ORF may result in gain-of-function or loss-of-function effects, respectively. Some upstream ORFs may encode a functional peptide, thereby regulating translation *in cis* through a sequence-dependent mechanism[29]. Our data indicate that the *U2HR*-encoded peptide negatively controls translation of the *HR* gene and implicate this sequence-dependent upstream ORF function in a human genetic disease. Furthermore, we showed that all loss-of-function mutations in *U2HR* could lead to increased translation of the main *HR* ORF, suggesting that the molecular mechanism underlying MUHH is gain of function of the *HR* gene. In the autosomal recessive congenital atrichia caused by loss-of-function mutations in *HR*[14–16], hair is shed almost completely within the first year of life and never regrows. On histopathological examination, the malformed hair follicles are often seen as keratinous follicular cysts. In the autosomal dominant MUHH, however, hair growth occurs during childhood, and severe hair loss occurs after puberty. Histopathological examination shows a marked reduction of hair follicles and various degrees of hair follicle atrophy[30]. Taken together with these facts, our work implicates the importance of fine-tuning the steady-state levels of HR protein in control of hair growth.

The HR protein is thought to have a crucial role in the telogen-anagen transition during hair follicle cycling[10]. A recent model linked the timing of HR protein expression and Wnt signaling in hair follicle regeneration[11]. The regulatory mechanisms by which the hair follicle cycle controls HR protein expression are largely unknown. The *U2HR*-encoded peptide may be a key factor in downregulating HR protein expression during anagen. In this sense, MUHH could be described as a condition with dysregulated, hair follicle cycle–dependent HR protein expression. Further studies on the regulatory role of the *U2HR* will shed light on the pathways controlling hair follicle cycle–dependent HR protein expression and offer a potential target for the development of therapeutic drugs to treat some forms of human hair loss or promote hair removal.

METHODS

Bioinformatics analysis. We examined a genomic region of 5 kb (chromosome 8, 22,041,880–22,046,879), centered by *HR* exon 1, on the human chromosome 8 reference sequence using the UCSC Genome Browser's human Mar.2006 assembly. The 'RefSeq Genes', 'Human ESTs' and 'Conservation' tracks were selected. The NCBI ORF Finder was used to find upstream ORFs in the *HR* 5′ UTR. Multiple sequence alignments of DNA and protein were carried out using ClustalW and WebLogo, respectively.

Linkage analysis. We collected blood samples from 18 members (11 affected, 3 unaffected and 4 spouse) of a five-generation Han Chinese family with MUHH, as well as another 24 families internationally. All patient samples were obtained with local institutional review board approval and written informed consent that complied with all principles of the Helsinki Accord. Genomic DNA was extracted by standard methods. For two-point linkage analysis, we typed four polymorphic microsatellite markers flanking the *HR* locus. Log_{10}-of-odds scores were calculated using the MLINK program of the LINKAGE package. The parameters used in linkage analysis were autosomal dominant inheritance, complete penetrance, a mutation rate of zero, equal male-female recombination rate, equal microsatellite-allele frequency and a disease-allele frequency of 1 in 10,000. PCR primers used for genotyping are given in **Supplementary Table 1** online.

Mutation screening. We screened three known genes in the crucial interval—*FGF17*, *HR* and *FAM160B2*—for pathogenic mutations in an affected individual of the above mentioned Chinese family. For *FGF17* and *FAM160B2*, we sequenced the coding exons and their flanking intronic sequences. In the case of *HR*, we PCR-amplified the whole genomic region into 16 overlapping fragments and sequenced them directly after purification. To confirm the 2T>C mutation in *U2HR*, we carried out genomic PCR using primers HRUP3F1 and HRUP3R1 and digested the products with the *Nco*I restriction enzyme. The digested products were separated on a 1.5% agarose gel along with the DL2,000 DNA Marker (TaKaRa). For mutation screening in other families with MUHH, PCR was carried out using the same primer pair, and the products were sequenced using HRUP3F1. PCR primers used for sequencing of *FGF17*, *HR* and *FAM160B2* are given in **Supplementary Table 1**.

Cloning and mutagenesis. We first introduced the *Eco*RI and *Sac*II cloning sites into the pGL3-Promoter plasmid by inserting at the *Hin*dIII/*Nco*I sites an annealed fragment of oligonucleotides A and B (**Supplementary Table 1**). The –642 to +81 cDNA fragment of *HR* was then cloned into the *Eco*RI/*Sac*II sites of the modified pGL3-Promoter plasmid to produce the pGL3-UTR-HR-Luc construct. A cDNA fragment containing the 2T>C or 104A>G *U2HR* mutation was obtained by PCR using genomic templates from affected individuals. The fragments were then used to replace to the corresponding wild-type one at the *Eco*RI and *Mlu*I sites of the pGL3-UTR-HR-Luc plasmid. All the other initiation codon mutations (in *U1HR*, *U3HR* and *U4HR*) and *U2HR* mutations (7C>T, 71T>A, 73C>G, 82G>C and 76G>A) were introduced individually into the parental pGL3-UTR-HR-Luc plasmid by PCR-mediated mutagenesis. To generate the HR-EGFP expression vectors, the *Eco*RI–*Sac*II insert from each pGL3-UTR-HR-Luc plasmid was subcloned into the same restriction sites of the pEGFP-N1 plasmid with a triple Flag tag inserted upstream of the ORF encoding Neo^r. All of the constructs were verified by sequencing. Primer sequences are given in **Supplementary Table 1**.

HR-luciferase reporter assay. HeLa cells were grown in DMEM supplemented with 10% FBS and transfected using Lipofectamine 2000 reagent (Invitrogen). A pGL3-UTR-HR-Luc plasmid was transfected into the cells growing in a 24-well plate, along with the pRL-TK *Renilla* luciferase vector, an internal control vector to normalize transfection efficiency. Twenty-four hours after transfection, cells were lysed and assayed for luciferase activity following the Dual-Luciferase protocol (Promega).

RT-PCR. We carried out RT-PCR in parallel with genomic PCR to confirm the *HR* 5′ UTR using templates from A375 and HeLa cells. For the HR-EGFP expression analysis, we applied quantitative real-time RT-PCR to detect the relative mRNA expression of the fused HR-EGFP. We transfected HeLa cells with an HR-EGFP expression plasmid and cultured the cells for 24 h. The two quantitative real-time RT-PCR assays for HR-EGFP and Flag-Neo^r were designed using Primer Express v2.0 software (Applied Biosystems). The two primer pairs were GFP-F and GFP-R and Neo-F and Neo-R (**Supplementary Table 1**). Quantitative PCR was carried out in a total volume of 20 µl, with each tube containing 10 µl of SYBR Premix Ex Taq (TaKaRa), 5 µl of reverse transcription product (50 ng) and 5 µl of primers (500 nM each). Four replicates were conducted per sample. Reactions were run in a Rotor-Gene 6000 real-time rotary analyzer (Corbett Life Science) at 95 °C for 10 min and then 40 cycles of 95 °C for 10 s, 60 °C for 15 s and 72 °C for 20 s. HR-EGFP mRNA expression was normalized to that of Neo^r, and the relative expression level was determined on the basis of the comparative $\Delta\Delta C_T$ method using the reverse transcription products from cells transfected with the wild-type HR-EGFP plasmid as the calibrator. The quantitative real-time RT-PCR experiments were repeated three times.

Immunoblot. Twenty-four hours after transfection, cells were washed twice in PBS and lysed in RIPA buffer (50 mM Tris-HCl, pH 7.4, 150 mM NaCl, 1% NP-40 and 0.1% SDS). Protein samples prepared from the transfected cells were separated using 12% Novex NuPAGE Tris-Bis gels (Invitrogen) and electro-blotted onto a polyvinylidene difluoride membrane (Millipore). After blocking in TBST buffer (10 mM Tris, pH 7.5, 150 mM NaCl and 0.5% Tween-20) containing 5% nonfat dried milk, blots were probed with mouse M2 monoclonal antibody to Flag (1:3,000; Sigma-Aldrich) followed by ImmunoPure peroxidase-conjugated goat antibody to mouse IgG (1:3,000; Pierce) and then developed with SuperSignal West Femto maximum sensitivity substrate. The same blots were stripped in 1% SDS with 25 mM glycine, pH 2.0, and reprobed with mouse monoclonal antibody to GFP (1:3,000; MBL).

Translation detection of U1HR and U2HR. To generate the U2HRno-stop construct, we inserted the –642 to –220 fragment of the *HR* 5′ UTR into the pEGFP-N1 plasmid, placing the *U2HR* upstream of and in frame with the ORF encoding EGFP. The U1HRno-stop construct was produced by cloning the –642 to –221 fragment of the *HR* 5′ UTR into the pEGFP-N1 plasmid and changing the termination codon TAG to CAG by PCR-mediated mutagenesis. These no-stop plasmids were individually transfected into HeLa cells, and the translated products were detected by immunoblot analysis using mouse monoclonal antibody to GFP (1:3,000; MBL) or custom-made rabbit polyclonal antibody to U2HR (1:3,000; AbMART).

URLs. UCSC Human Genome Browser Gateway, http://genome.ucsc.edu/; NCBI ORF Finder, http://www.ncbi.nlm.nih.gov/gorf/gorf.html; WebLogo, http://weblogo.berkeley.edu.

Accession codes. GenBank: *HR*, NM_005144; *FGF17*, NM_003867; *FAM160B2*, NM_022749.

Note: Supplementary information is available on the Nature Genetics website.

ACKNOWLEDGMENTS

We thank the family members for their participation in the study, and J. Zeller, S. Burge and M. Young for referring patients. This work was supported mainly by the National Natural Science Foundation of China (funds 30730097 and 30721063 to X.Z.). X.Z. is a Chang Jiang Scholar of Genetic Medicine supported by the

Ministry of Education, China. C.-D.H. was supported by the National Natural Science Foundation of China (30771948). The McLean laboratory is supported by grants from the Dystrophic Epidermolysis Bullosa Research Association, the Pachyonychia Congenita Project, the British Skin Foundation, the National Eczema Society and the Medical Research Council (G0700314). S.Y. is supported by the Ministry of Education, China (SRFDP 20050366004). The German group is supported by grants from the Deutsche Forschungsgemeinschaft (Research Unit FOR 423 to M.M.N. and R.K. and Emmy Noether Programme to R.C.B.). M.M.N. holds an Alfried Krupp von Bohlen and Halbach-Chair in Genetic Medicine. R.S. and J.G. are supported by Epiderm, the Scientific Research Fund of the Australasian College of Dermatologists and the Scientific Research Fund of the Skin and Cancer Foundation of Victoria.

AUTHOR CONTRIBUTIONS

X.Z. designed and oversaw the entire project. X.Z. and C.-D.H. initiated the study. X.Z. and W.H.I.M. coordinated the mutation screening work and prepared the manuscript. Y.W., Y. Liu, Y.Z. and M.v.G. carried out the linkage analysis and mutation screening. Y.X., R.H., K.W. and Y.W. conducted the mRNA and protein expression experiments. X.Z. and Y.W. conducted the bioinformatics analysis. M.S., D.S., Q.L., Y. Luo and L.J. supported the genetic analyses. H.-D.C. and W.H.-Y.L. supported the study design. Y. Liu, S.Y., X.-J.Z., R.K., S.C., R.C.B., M.M.N., M.A.M.v.S., P.M.S., D.H., M.H., G.S.D., C.K., A.M., C.S.M., A.T., A.H., C.B., Y.d.P., A.S.P., A.D.I., R.S. and J.G. were responsible for clinical evaluation and sample collection, including earlier published linkage studies.

COMPETING INTERESTS STATEMENT

The authors declare competing financial interests: details accompany the full-text HTML version of the paper at http://www.nature.com/naturegenetics/.

Published online at http://www.nature.com/naturegenetics/
Reprints and permissions information is available online at http://npg.nature.com/reprintsandpermissions/

1. Paus, R. & Cotsarelis, G. The biology of hair follicles. *N. Engl. J. Med.* **341**, 491–497 (1999).
2. Stenn, K.S. & Paus, R. Controls of hair follicle cycling. *Physiol. Rev.* **81**, 449–494 (2001).
3. Cotsarelis, G. Epithelial stem cells: a folliculocentric view. *J. Invest. Dermatol.* **126**, 1459–1468 (2006).
4. Alonso, L. & Fuchs, E. Stem cells in the skin: waste not, Wnt not. *Genes Dev.* **17**, 1189–1200 (2003).
5. Huelsken, J., Vogel, R., Erdmann, B., Cotsarelis, G. & Birchmeier, W. beta-Catenin controls hair follicle morphogenesis and stem cell differentiation in the skin. *Cell* **105**, 533–545 (2001).
6. Andl, T., Reddy, S.T., Gaddapara, T. & Millar, S.E. WNT signals are required for the initiation of hair follicle development. *Dev. Cell* **2**, 643–653 (2002).
7. Van Mater, D., Kolligs, F.T., Dlugosz, A.A. & Fearon, E.R. Transient activation of beta-catenin signaling in cutaneous keratinocytes is sufficient to trigger the active growth phase of the hair cycle in mice. *Genes Dev.* **17**, 1219–1224 (2003).
8. Ito, M. *et al.* Wnt-dependent de novo hair follicle regeneration in adult mouse skin after wounding. *Nature* **447**, 316–320 (2007).
9. Potter, G.B. *et al.* The hairless gene mutated in congenital hair loss disorders encodes a novel nuclear receptor corepressor. *Genes Dev.* **15**, 2687–2701 (2001).
10. Beaudoin, G.M. III, Sisk, J.M., Coulombe, P.A. & Thompson, C.C. Hairless triggers reactivation of hair growth by promoting Wnt signaling. *Proc. Natl. Acad. Sci. USA* **102**, 14653–14658 (2005).
11. Thompson, C.C., Sisk, J.M. & Beaudoin, G.M. III. Hairless and Wnt signaling: allies in epithelial stem cell differentiation. *Cell Cycle* **5**, 1913–1917 (2006).
12. Ahmad, W. *et al.* Alopecia universalis associated with a mutation in the human hairless gene. *Science* **279**, 720–724 (1998).
13. Cichon, S. *et al.* Cloning, genomic organization, alternative transcripts and mutational analysis of the gene responsible for autosomal recessive universal congenital alopecia. *Hum. Mol. Genet.* **7**, 1671–1679 (1998).
14. Sprecher, E., Bergman, R., Szargel, R., Friedman-Birnbaum, R. & Cohen, N. Identification of a genetic defect in the hairless gene in atrichia with papular lesions: evidence for phenotypic heterogeneity among inherited atrichias. *Am. J. Hum. Genet.* **64**, 1323–1329 (1999).
15. Unna, M. Über hypotrichosis congenita hereditaria. *Dermatol. Wochenschr.* **81**, 1167–1178 (1925).
16. van Steensel, M. *et al.* The gene for hypotrichosis of Marie Unna maps between D8S258 and D8S298: exclusion of the hr gene by cDNA and genomic sequencing. *Am. J. Hum. Genet.* **65**, 413–419 (1999).
17. Sreekumar, G.P., Roberts, J.L., Wong, C.Q., Stenn, K.S. & Parimoo, S. Marie Unna hereditary hypotrichosis gene maps to human chromosome 8p21 near hairless. *J. Invest. Dermatol.* **114**, 595–597 (2000).
18. Lefevre, P. *et al.* Linkage of Marie-Unna hypotrichosis locus to chromosome 8p21 and exclusion of 10 genes including the hairless gene by mutation analysis. *Eur. J. Hum. Genet.* **8**, 273–279 (2000).
19. Cichon, S. *et al.* A distinct gene close to the hairless locus on chromosome 8p underlies hereditary Marie Unna type hypotrichosis in a German family. *Br. J. Dermatol.* **143**, 811–814 (2000).
20. He, P.P. *et al.* Refinement of a locus for Marie Unna hereditary hypotrichosis to a 1.1-cM interval at 8p21.3. *Br. J. Dermatol.* **150**, 837–842 (2004).
21. Scheper, G.C., van der Knaap, M.S. & Proud, C.G. Translation matters: protein synthesis defects in inherited disease. *Nat. Rev. Genet.* **8**, 711–723 (2007).
22. Cazzola, M. & Skoda, R.C. Translational pathophysiology: a novel molecular mechanism of human disease. *Blood* **95**, 3280–3288 (2000).
23. Wiestner, A., Schlemper, R.J., van der Maas, A.P. & Skoda, R.C. An activating splice donor mutation in the thrombopoietin gene causes hereditary thrombocythaemia. *Nat. Genet.* **18**, 49–52 (1998).
24. Liu, L. *et al.* Mutation of the CDKN2A 5′ UTR creates an aberrant initiation codon and predisposes to melanoma. *Nat. Genet.* **21**, 128–132 (1999).
25. Panteleyev, A.A., Paus, R. & Christiano, A.M. Patterns of hairless (hr) gene expression in mouse hair follicle morphogenesis and cycling. *Am. J. Pathol.* **157**, 1071–1079 (2000).
26. Yang, S. *et al.* Identification of a novel locus for Marie Unna hereditary hypotrichosis to a 17.5 cM interval at 1p21.1–1q21.3. *J. Invest. Dermatol.* **125**, 711–714 (2005).
27. Iacono, M., Mignone, F. & Pesole, G. uAUG and uORFs in human and rodent 5′untranslated mRNAs. *Gene* **349**, 97–105 (2005).
28. Churbanov, A., Rogozin, I.B., Babenko, V.N., Ali, H. & Koonin, E.V. Evolutionary conservation suggests a regulatory function of AUG triplets in 5′-UTRs of eukaryotic genes. *Nucleic Acids Res.* **33**, 5512–5520 (2005).
29. Sachs, M.S. & Geballe, A.P. Downstream control of upstream open reading frames. *Genes Dev.* **20**, 915–921 (2006).
30. Niiyama, S., Freyschmidt-Paul, P., Happle, R. & Hoffmann, R. Hypotrichosis of congenital of Marie Unna. *Eur. J. Dermatol.* **11**, 379–380 (2001).